PRESTAZIONE SISMICA DI PONTI ISOLATI CON DISPOSITIVI ATTRITIVI A DOPPIA SUPERFICIE: UN'ANALISI PARAMETRICA

SEISMIC PERFORMANCE OF BRIDGES ISOLATED BY DCFP DEVICES: A PARAMETRIC ANALYSIS

Paolo Castaldo, Guglielmo Amendola, Luca Giordano,
Elena Miceli, Diego Gino
Politecnico di Torino
Department of Structural, Geotechnical and Buildings Engineering
Turin, Italy
paolo.castaldo@polito.it; guglielmo.amendola@polito.it; luca.giordano@polito.it;
elena.miceli@polito.it; diego.gino@polito.it

ABSTRACT

The present investigation examines how the properties of the double concave friction pendulum (DCFP) devices influence the seismic performance of isolated multi-span continuous deck bridges. The numerical simulations are carried out using an eight-degree-of-freedom model to reproduce the elastic behavior of the pier, associated to the assumption of both rigid abutment and rigid deck, and the non-linear velocity-dependent behavior of the two surfaces of the double concave friction pendulum isolators under a set of natural records with different characteristics. The results in terms of the statistics related to the relevant response parameters are computed in non-dimensional form with respect to the seismic intensity considering different properties of both DCFP isolators and bridge.

SOMMARIO

Il presente studio esamina come le proprietà degli isolatori attritivi a doppia superficie (Double Concave Friction Pendulum) influenzano le prestazioni sismiche di ponti a impalcato continuo a più campate. Le simulazioni numeriche sono effettuate utilizzando un modello a otto gradi di libertà per riprodurre il comportamento elastico della pila, associato all'assunzione sia di spalla rigida che di impalcato rigido, e il comportamento non lineare dipendente dalla velocità delle due superfici degli isolatori attritivi sotto una serie di eventi sismici naturali con caratteristiche diverse. I risultati in termini di statistiche relative ai parametri di risposta rilevanti sono calcolati in forma non

dimensionale rispetto all'intensità sismica considerando differenti proprietà sia degli isolatori che del ponte.

1   INTRODUCTION

One of the main goals of seismic isolation is to enrich the performance of structures [1]-[2] and infrastructure [3] when subjected to seismic loading. The safety level associated with both structures [4] and infrastructures turns out to be a key aspect especially in seismic-prone areas.

As a matter of fact, the non-linear behaviour of reinforced concrete (RC) elements strongly influences the overall seismic response when no isolation systems are provided. With a special reference to bridges, is it well known in the literature that seismic isolation allows to threat the superstructure and the substructure as a decoupled system, with a consequent reduction of the transmitted forces in case of an earthquake. Many research efforts have been carried out to study the influence of the installation of isolator devices on the bridges [5]. Particularly, numerous studies [7] have been focused on seismic isolation through friction pendulum systems (FPS). One of the greatest advantages of using FPS devices is the significant energy dissipation that occurs under seismic action, along with its recentering capability; furthermore, they make the natural period of the isolated bridge independent from the deck mass [8]. These devices can have single or multiple concave sliding surfaces [9]-[11]. Among those having multiple surfaces, the adoption of double concave sliding surface friction pendulum (DCFP) systems has shown to have a more positive influence on the seismic isolation of bridges [12]-[13]. Following this isolation approach, the present work presents a parametric analysis of multi-span continuous bridges isolated with DCFP devices, where the interaction between abutments, pier and deck [14] is also taken into account. The bridge model is performed following an eight-degree-of-freedom (8-dof) system approximation. This simplification can be reasonably representative of real bridges similar to those investigated. The adopted model accounts for the RC pier stiffness, the RC rigid abutments and the DCFP devices behavior. To explicitly consider the uncertainties related to the so-called record-to-record variability, 30 different ground motions have been considered to perform all the analyses. In addition, the geometric configuration of the pier and of the DCFP isolators are parametrically investigated. The maximum response of the deck and of the pier are identified and statistically post processed to evaluate their seismic performance as a function of the varying parameters. Finally, an optimum design value of the friction coefficient, i.e. able to minimize the pier top maximum displacement, is analyzed and provided into a regression model.

2   DYNAMIC RESPONSE OF THE DECK-ABUTMENT-PIER STRUCTURAL SYSTEM

The 8-degree-of-freedom (8-dof) system model as approximation of the three-span continuous deck bridge isolated with DPCF is shown in Fig. 1. In particular, 5 dofs are used to model the lumped masses of the elastic RC pier, while 2 dofs model DPCF devices and 1 dof is adopted for the rigid RC deck [6].
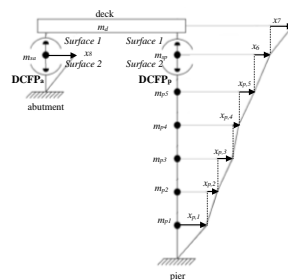

Fig. 1. Schematic illustration for the 8-dof model of the bridge.

From the dynamic equilibrium of the multi-degree of freedom system depicted in Fig.1 the equations of motion governing the seismic problem can be expressed in terms of drift between the lumped masses along the longitudinal direction as follows:

$$m_d\ddot{x}_7(t) + m_d\ddot{x}_6(t) + m_d\ddot{x}_{p5}(t) + m_d\ddot{x}_{p4}(t) + m_d\ddot{x}_{p3}(t) + m_d\ddot{x}_{p2}(t) + m_d\ddot{x}_{p1}(t)$$
$$+ c_d\dot{x}_d(t) + F_{1a}(t) + F_{1p}(t) = -m_d\ddot{u}_g(t)$$

$$m_{sp}\ddot{x}_6(t) + m_{sp}\ddot{x}_{p5}(t) + m_{sp}\ddot{x}_{p4}(t) + m_{sp}\ddot{x}_{p3}(t) + m_{sp}\ddot{x}_{p2}(t) + m_{sp}\ddot{x}_{p1}(t)$$
$$- F_{1p}(t) + F_{2p}(t) = -m_{sp}\ddot{u}_g(t)$$

$$m_{sa}\ddot{x}_8(t) - F_{1a}(t) + F_{2a}(t) = -m_{sa}\ddot{u}_g(t)$$

$$m_{p5}\ddot{x}_{p5}(t) + m_{p5}\ddot{x}_{p4}(t) + m_{p5}\ddot{x}_{p3}(t) + m_{p5}\ddot{x}_{p2}(t) + m_{p5}\ddot{x}_{p1}(t) - c_d\dot{x}_d(t)$$
$$+ c_{p5}\dot{x}_{p5}(t) + k_{p5}x_{p5}(t) - F_{2p}(t) = -m_{p5}\ddot{u}_g(t)$$

$$m_{p4}\ddot{x}_{p4}(t) + m_{p4}\ddot{x}_{p3}(t) + m_{p4}\ddot{x}_{p2}(t) + m_{p4}\ddot{x}_{p1}(t) - c_{p5}\dot{x}_{p5}(t) - k_{p5}x_{p5}(t)$$
$$+ c_{p4}\dot{x}_{p4}(t) + k_{p4}x_{p4}(t) = -m_{p4}\ddot{u}_g(t)$$
$$\qquad\qquad (1)$$

$$m_{p3}\ddot{x}_{p3}(t) + m_{p3}\ddot{x}_{p2}(t) + m_{p3}\ddot{x}_{p1}(t) - c_{p4}\dot{x}_{p4}(t) - k_{p4}x_{p4}(t) + c_{p3}\dot{x}_{p3}(t)$$
$$+ k_{p3}x_{p3}(t) = -m_{p3}\ddot{u}_g(t)$$

$$m_{p2}\ddot{x}_{p2}(t) + m_{p2}\ddot{x}_{p1}(t) - c_{p3}\dot{x}_{p3}(t) - k_{p3}x_{p3}(t) + c_{p2}\dot{x}_{p2}(t) + k_{p2}x_{p2}(t)$$
$$= -m_{p2}\ddot{u}_g(t)$$

$$m_{p1}\ddot{x}_{p1}(t) - c_{p2}\dot{x}_{p2}(t) - k_{p2}x_{p2}(t) + c_{p1}\dot{x}_{p1}(t) + k_{p1}x_{p1}(t) = -m_{p1}\ddot{u}_g(t)$$

where m_d, m_{sp}, and m_{sa} are respectively the masses of the deck and of the two isolation devices installed on the pier and on the abutment ; m_{pi} (i=1,..,4,5) is the i-th lumped mass of the pier segment; k_{pi} and c_{pi} (i=1,..,5) are the stiffness and viscous damping, assumed equal for each dof associated to the pier segments; t is the time instant; $F_{ja}(t)$ and $F_{jp}(t)$ are the reaction forces of the DCFP referred to the abutment and the pier, respectively, for the upper ($j = 1$) and lower sliding surface ($j = 2$). In particular, according to [9]-[11], the reaction forces can be expressed as:

$$F_{1a} = \frac{m_d g}{2}\left[\frac{1}{R_{1a}}\left(\sum_{i=1}^{5} x_{pi} + x_6 + x_7 - x_8\right) + \mu_{1a}(\dot{x}_9)(sgn(\dot{x}_9))\right]$$

$$F_{2a} = \left(\frac{m_d}{2} + m_{sa}\right)g\left[\frac{1}{R_{2a}}(x_8) + \left(\mu_{2a}(\dot{x}_8)\right)(sgn(\dot{x}_8))\right]$$
$$\qquad\qquad (2)$$

$$F_{1p} = \left(\frac{m_d g}{2}\right)\left[\frac{1}{R_{1p}}(x_7) + \left(\mu_{1p}(\dot{x}_7)\right)(sgn(\dot{x}_7))\right]$$

$$F_{2p} = \left(\frac{m_d}{2} + m_{sp}\right)g\left[\frac{1}{R_{2p}}(x_6) + \left(\mu_{2p}(\dot{x}_6)\right)(sgn(\dot{x}_6))\right]$$

where $x_9 = \sum_{i=1}^{5} x_{pi} + x_6 + x_7 - x_8$, R_1 and R_2 are the upper and lower radius of curvature of the DCFP devices and $\mu_j(\dot{x}_j(t))$ (with j=1,2) is the sliding friction coefficient, estimated according to experimental investigation [16]-[18] with the following expression:

$$\mu_j(\dot{x}_j) = f_{j,max} - (f_{j,max} - f_{j,min})\cdot exp(-\alpha|\dot{x}_j|) \qquad\qquad (3)$$

where $f_{j,max}$ and $f_{j,min}$ are the value of friction coefficient at high and near-zero sliding velocity respectively. Finally it is assumed α=30 and $f_{j,max}=3\,f_{j,min}$ according to [16]-[18]. Then, in line with previous studies [19], the system in (1) can be expressed in a non-dimensional form, by means of mass ratios; the circular frequency of vibration of the isolated deck and of the i-th dof of the pier; the damping coefficient of the i-th dof of the pier, respectively as:

$$\lambda_{pi} = \frac{m_{pi}}{m_d}, \lambda_{sa} = \frac{m_{sa}}{m_d}, \lambda_{sp} = \frac{m_{sp}}{m_d}, \omega_d = \sqrt{\frac{k_{comb}}{m_d}}, \omega_{pi} = \sqrt{\frac{k_{pi}}{m_{pi}}}, \xi_{pi} = \frac{c_{pi}}{2m_{pi}\omega_{pi}} \qquad (4)$$

In addition, according to [19], the time scale $\tau=t\omega_d$ can be introduced together with the seismic intensity scale factor a_0, evaluated with the expression $\ddot{u}_g(t) = a_0\ell(\tau)$, where $\ell(\tau)$ is a non-dimensional function of time which describes the time history of the seismic event. Finally, the non-dimensional system of equations becomes:

$$\ddot{\psi}_7(\tau) + \ddot{\psi}_6(\tau) + \ddot{\psi}_{p5}(\tau) + \ddot{\psi}_{p4}(\tau) + \ddot{\psi}_{p3}(\tau) + \ddot{\psi}_{p2}(\tau) + \ddot{\psi}_{p1}(\tau) + 2\xi_d\dot{\psi}_7(\tau) +$$

$$\frac{g}{2}\left[\frac{1}{R_{1p}}\frac{1}{\omega_d^2}\psi_7(\tau) + \frac{\mu_{1p}(\dot{\psi}_7)}{a_0}sgn(\dot{\psi}_7)\right] + \frac{g}{2}\left[\frac{1}{R_{1a}}\frac{1}{\omega_d^2}\left(\sum_{i=1}^{5}\psi_{pi}(\tau) + \psi_6(\tau) + \psi_7(\tau) - \psi_8(\tau)\right) + \right.$$

$$\left. + \left(\frac{\mu_{1a}(\dot{\psi}_9)}{a_0}\right)\left(sgn\left(\sum_{i=1}^{5}\dot{\psi}_{pi}(\tau) + \dot{\psi}_6(\tau) + \dot{\psi}_7(\tau) - \dot{\psi}_8(\tau)\right)\right)\right] = -\ell(\tau)$$

$$\lambda_{sp}[\ddot{\psi}_6(\tau) + \ddot{\psi}_{p5}(\tau) + \ddot{\psi}_{p4}(\tau) + \ddot{\psi}_{p3}(\tau) + \ddot{\psi}_{p2}(\tau) + \ddot{\psi}_{p1}(\tau)]$$

$$- \frac{g}{2}\left[\frac{1}{R_{1p}}\frac{1}{\omega_d^2}\psi_7(\tau) + +\frac{\mu_{1p}(\dot{\psi}_7)}{a_0}sgn(\dot{\psi}_7)\right]$$

$$+ \left(\frac{1}{2} + \lambda_{sp}\right)g\left[\frac{1}{R_{2p}}\frac{1}{\omega_d^2}\psi_6(\tau) + \frac{\mu_{2p}(\dot{\psi}_6)}{a_0}sgn(\dot{\psi}_6)\right] = -\lambda_{sp}\ell(\tau)$$

$$\lambda_{sa}\ddot{\psi}_8(\tau) - \frac{g}{2}\left[\frac{1}{R_{1a}}\frac{1}{\omega_d^2}\left(\sum_{i=1}^{5}\psi_{pi}(\tau) + \psi_6(\tau) + \psi_7(\tau) + -\psi_8(\tau)\right) + \left(\frac{\mu_{1a}(\dot{\psi}_9)}{a_0}\right)\left(sgn\left(\sum_{i=1}^{5}\dot{\psi}_{pi}(\tau) + \right.\right.\right.$$

$$\left.\left.\left. \dot{\psi}_6(\tau) + \dot{\psi}_7(\tau) - \dot{\psi}_8(\tau)\right)\right)\right] +$$

$$+ \left(\frac{1}{2} + \lambda_{sa}\right)g\left[\frac{1}{R_{2a}}\frac{1}{\omega_d^2}\psi_8(\tau) + \frac{\mu_{2a}(\dot{\psi}_8)}{a_0}sgn(\dot{\psi}_8)\right] = -\lambda_{sa}\ell(\tau)$$

$$\lambda_{p5}[\ddot{\psi}_{p5}(\tau) + \ddot{\psi}_{p4}(\tau) + \ddot{\psi}_{p3}(\tau) + \ddot{\psi}_{p2}(\tau) + \ddot{\psi}_{p1}(\tau)] - 2\xi_d\dot{\psi}_d(\tau) + 2\xi_{p5}\lambda_{p5}\frac{\omega_{p5}}{\omega_d}\dot{\psi}_{p5}(\tau) +$$

$$+ \frac{\lambda_{p5}\omega_{p5}^2}{\omega_d^2}\psi_{p5}(\tau) - \left(\frac{1}{2} + \lambda_{sp}\right)g\left[\frac{1}{R_{2p}}\frac{1}{\omega_d^2}\psi_6(\tau) + \frac{\mu_{2p}(\dot{\psi}_6)}{a_0}sgn(\dot{\psi}_6)\right] = -\lambda_{p5}\ell(\tau)$$

$$\lambda_{p4}[\ddot{\psi}_{p4}(\tau) + \ddot{\psi}_{p3}(\tau) + \ddot{\psi}_{p2}(\tau) + \ddot{\psi}_{p1}(\tau)] - 2\xi_{p5}\lambda_{p5}\frac{\omega_{p5}}{\omega d}\dot{\psi}_{p5}(\tau) + 2\xi_{p4}\lambda_{p4}\frac{\omega_{p4}}{\omega d}\dot{\psi}_{p4}(\tau) +$$

$$-\lambda_{p5}\frac{\omega_{p5}^2}{\omega_d^2}\psi_{p5}(\tau) + +\lambda_{p4}\frac{\omega_{p4}^2}{\omega_d^2}\psi_{p4}(\tau) = -\lambda_{p4}\ell(\tau)$$

$$\lambda_{p3}[\ddot{\psi}_{p3}(\tau) + \ddot{\psi}_{p2}(\tau) + \ddot{\psi}_{p1}(\tau)] - 2\xi_{p4}\lambda_{p4}\frac{\omega_{p4}}{\omega d}\dot{\psi}_{p4}(\tau) + 2\xi_{p3}\lambda_{p3}\frac{\omega_{p3}}{\omega d}\dot{\psi}_{p3}(\tau) + -\lambda_{p4}\frac{\omega_{p4}^2}{\omega_d^2}\psi_{p4}(\tau) +$$

$$\lambda_{p3}\frac{\omega_{p3}^2}{\omega_d^2}\psi_{p3}(\tau) = -\lambda_{p3}\ell(\tau)$$

$$\lambda_{p2}[\ddot{\psi}_{p2}(\tau) + \ddot{\psi}_{p1}(\tau)] - 2\xi_{p3}\lambda_{p3}\frac{\omega_{p3}}{\omega d}\dot{\psi}_{p3}(\tau) + 2\xi_{p2}\lambda_{p2}\frac{\omega_{p2}}{\omega_d}\dot{\psi}_{p2}(\tau) - \lambda_{p3}\frac{\omega_{p3}^2}{\omega_d^2}\psi_{p3}(\tau)$$

$$+ \lambda_{p2}\frac{\omega_{p2}^2}{\omega_d^2}\psi_{p2}(\tau) = -\lambda_{p2}\ell(\tau)$$

$$\lambda_{p1}\ddot{\psi}_{p1}(\tau) - 2\xi_{p2}\lambda_{p2}\frac{\omega_{p2}}{\omega d}\dot{\psi}_{p2}(\tau) + 2\xi_{p1}\lambda_{p1}\frac{\omega_{p1}}{\omega_d}\dot{\psi}_{p1}(\tau) - \lambda_{p2}\frac{\omega_{p2}^2}{\omega_d^2}\psi_{p2}(\tau) + \lambda_{p1}\frac{\omega_{p1}^2}{\omega_d^2}\psi_{p1}(\tau)$$

$$= -\lambda_{p1}\ell(\tau)$$

$$(5)$$

with the following non-dimensional parameters:

$$\Pi_{\omega i} = \frac{\omega_{pi}}{\omega_d}, \Pi_{\lambda i} = \lambda_{pi} = \frac{m_{pi}}{m_d}, \Pi_{\lambda sa} = \lambda_{sa}$$

$$\Pi_{\lambda sp} = \lambda_{sp}, \Pi_{\mu 1a}(\dot{\psi}_9) = \frac{\mu_{1a}(\dot{\psi}_9)g}{a_0}, \Pi_{\mu 1p}(\dot{\psi}_7) = \frac{\mu_{1p}(\dot{\psi}_7)g}{a_0} \qquad (6)$$

$$\Pi_{\mu 2a}(\dot{\psi}_8) = \frac{\mu_{2a}(\dot{\psi}_8)g}{a_0}, \Pi_{\mu 2p}(\dot{\psi}_6) = \frac{\mu_{2p}(\dot{\psi}_6)g}{a_0}, \Pi_{\xi_{pi}} = \xi_{p_i}$$

In the end, the maximum response in terms of non-dimensional parameters is evaluated as:

$$\Psi_{u_d} = \frac{u_{d,max} \cdot \omega_d^2}{a_0}, \Psi_{u_p} = \frac{u_{p,max} \cdot \omega_d^2}{a_0} = \frac{\left(\sum_{i=1}^5 x_i\right)_{max} \cdot \omega_d^2}{a_0}, \Psi_{x_d} = \frac{x_{d,max} \cdot \omega_d^2}{a_0} = \frac{(x_6+x_7)_{max} \cdot \omega_d^2}{a_0} \quad (7)$$

3 PARAMETRIC ANALYSIS OF THE STRUCTURAL SEISMIC RESPONSE

In the following, the outcomes of the performed parametric analysis for the bridge isolated with DCFP bearings are provided in terms of non-dimensional parameters.

3.1 Selection of the seismic inputs

Following the performance-based earthquake engineering (PBEE) framework [20], the uncertainties related to the seismic input intensity are separated from the ones related to the characteristics of the record (i.e., record-to-record variability) by introducing an intensity measure (IM). For the specific case, the IM corresponds to the seismic intensity scale factor a_0. In this specific application also, to reach efficiency, sufficiency and hazard compatibility criteria [21], the spectral pseudo-acceleration, $S_A(T_d)$ function of the isolated period of the system (i.e., $T_d=2\pi/\omega_d$), is adopted as intensity measure IM. This implies assuming $a_0 = S_A(T_d)$. As stayed above, the record-to-record variability is described through a set of 30 ground motion records as reported in [19]-[22].

3.2 Probabilistic analysis of the seismic response

In the present investigation, the maximum structural response variables considered are the following: the *maximum deck response* $u_{d,max}$, which correspondes to the maximum isolator global response on the abutment; the *maximum displacement at the top of the pier* $u_{p,max}$ relative to the ground. By solving the Eq. (5), these responses can be evaluated as a function of the selected set of records, in non-dimensional form. According to the PBEE method [23], the non-dimensional response parameters may be assumed lognormally distributed. The statistical parameters for lognormal distribution can be derived from the generic response parameter D (i.e., the maximum values of ψ_{u_d}, ψ_{x_p} and ψ_{u_p} expressed in (7)) by estimating the mean value *GM(D)* and the coefficient of variation *β(D)* of the observed samples calculated as in [19].

Finally, being valid the lognormality assumption, the *k*-th percentile of the generic response parameter *D* can be derived as follows:

$$d_k = GM(D) \, exp[\, f(k)\beta(D)] \quad (8)$$

where *f(k)* is equal to *f(50)=0* and f(84)=1 for the 50-th and 84-percentiles, respectively [24].

3.3 Results of the parametric analysis

The parametric analysis reported herein evaluates how the DCFP devices' properties, as well as the bridge geometry, influence the overall seismic performance of the structures or infrastrucutres, subjected to seismic loading. In particular: the non-dimensional parameters for the damping factor $\Pi_{\xi_d} = \xi_d$ and $\Pi_{\xi_p} = \xi_p$ are assumed equal to 0% and 5% respectively; the RC pier period T_p is constant and equal to 0.2s [12]; the isolated bridge period T_d is parametrically investigated as follows: 2s, 2.5s, 3s, 3.5s, 4s; the five pier lumped masses $\Pi_\lambda=\lambda_P$ are equal to 0.1, 0.15 and 0.2 [12]; the two DCFP isolators on the abutment and on the pier have identical properties (i.e., $\Pi^*_{\mu_{1a}} = \Pi^*_{\mu_{1p}} = \Pi^*_{\mu_1}$ and $\Pi_{\lambda S_a} = \Pi_{\lambda S_p} = \Pi_{\lambda S}$. The DCFP bearing main properties are the following: $R_1/R_2=2$, $\mu_{1,max}/\mu_{2,max}=2$, $\mu_{j,max}/\mu_{j,min}=3$, with (j=1,2).

For the parameter $\Pi^*_{\mu_1}$, 80 values are considered in the range between 0 (no friction) and 2 (very high friction). Following the non-dimensional parametric approach, a suite of 1200 different configurations is considered, by solving the equation of motion in (5) for the 30 different ground

motions. To do so, the integration algorithm *Bogacki-Shampine* in Matlab-Simulink [25] has been used. In the following (Fig. 2,3), the statical parameters in terms of GM and β of the non-dimensional maximum responses are shown, as a function of the system properties. In each figure, three different surface plots are present, each of them corresponding to a value of Π_λ. Fig. 2 illustrates the maximum normalized displacement of the pier top with respect to the ground (i.e., ψ_{u_p}). Regarding the mean Fig. 2 (left), for very low $\Pi^*_{\mu_1}$ values, $GM(\psi_{u_p})$ decreases by increasing $\Pi^*_{\mu_1}$, and sligthly increases for high $\Pi^*_{\mu_1}$ values. This suggests that an optimal value for the $\Pi^*_{\mu_1}$ parameter can be achieved by minimizing the pier top maximum displacement. This optimal value varies in the range 0 and 0.5 as function of the values assumed by the isolated deck period T_d and the pier lumped masses factor Π_λ. Moreover, the mean value of ψ_{u_p} decreases significantly with increasing Π_λ. Regarding the dispersion Fig. 2 (right), the maximum value of $\beta(\psi_{u_p})$ is in the same range of $\Pi^*_{\mu_1}$ that gives the minimization of the mean value $GM(\psi_{u_p})$. In addition, $\beta(\psi_{u_p})$ increases with larger mass ratios Π_λ.
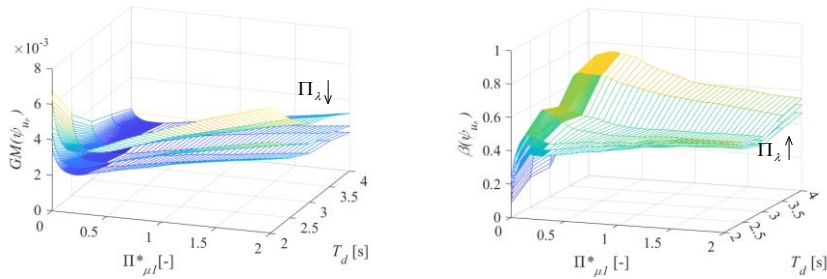
Fig. 2. Pier top normalized displacement ψ_{u_p} vs. $\Pi^*_{\mu_1}$ and T_d for T_p =0.05s and for Π_λ=0.1,0.15,0.2 left) mean value; right) dispersion.

The optimal values for the dimensionless friction parameter $\Pi^*_{\mu,opt}$ can be used for multivariate non-linear regression analysis. This allows providing an optimal value for any combination of the main dynamic characteristics of an isolated bridge. As a matter of fact this expression may be used in both design or retrofit of an existing bridge, and its reliability is given by the R^2 coefficient as reported in Table 1 along with the overall results of the regression analyses. A quadratic regression law has been calculated trough an ad-hoc Matlab routine for the different percentiles and the dimensionless pier displacement as follows:

$$\Pi^*_{\mu,optimum}\left(\psi_{u_p}\left(50^{th}, 84^{th}\right) = c_1 + c_2 \frac{T_p}{T_d} + c_3 T_p^2 + c_4 \frac{T_p}{\Pi_\lambda} + c_5 \frac{T_p^3}{T_d} + c_6 \frac{T_p}{T_d \Pi_\lambda} + c_7 \frac{T_p^3}{\Pi_\lambda} + $$
$$+ c_8 \left(\frac{T_p}{T_d}\right)^2 + c_9 T_p^4 + c_{10} \left(\frac{T_p}{\Pi_\lambda}\right)^2$$

$$\psi_{u_p}\left(50^{th}, 84^{th}\right) = c_1 + c_2 \frac{T_p}{T_d} + c_3 T_p^2 + c_4 \frac{T_p}{\Pi_\lambda} + c_5 \frac{T_p^3}{T_d} + c_6 \frac{T_p}{T_d \Pi_\lambda} + c_7 \frac{T_p^3}{\Pi_\lambda} + c_8 \left(\frac{T_p}{T_d}\right)^2 \qquad (9)$$
$$+ c_9 T_p^4 + c_{10} \left(\frac{T_p}{\Pi_\lambda}\right)^2$$

Fig. 3 shows the statistics for the normalized maximum deck displacement ψ_{u_d}, which also corresponds to the maximum global response of the bearing placed on the abutment. The mean value Fig. 3 (left) $GM(\psi_{u_d})$ decreases significantly as $\Pi^*_{\mu_1}$ increases. In addition, the values of $GM(\psi_{u_d})$ slightly increase for larger values of Π_λ. The values of the dispersion $\beta(\psi_{u_d})$, represented in Fig. 3 (right), are very low for low $\Pi^*_{\mu_1}$ values due to the high efficiency of the *IM*, and attain their peak for high values of $\Pi^*_{\mu_1}$.

Table 1. Regression statistics for the friction and pier's top displacement

	$\Pi^*_{\mu,opt}(50^{th})$	$\psi_{u_p}(50^{th})$	$\Pi^*_{\mu,opt}(84^{th})$	$\psi_{u_p}(84^{th})$
R^2	0.8300803	0.995616	0.667019	0.986492
c_1	0.3553902	0.002046	0.412809	0.007069
c_2	-7.1923149	-0.249568	2.428517	-0.833586
c_3	34.315356	1.22837	16.0888	3.490969
c_4	-0.2680317	-0.00474	-0.299282	-0.011717
c_5	-43.21174	-14.67963	1091.082	-48.45321
c_6	5.8143672	0.265643	-7.451915	0.332688
c_7	-7.2993286	-0.283925	7.95924	-0.846431
c_8	-19.247373	5.065239	-221.9676	16.29055
c_9	-269.04039	13.08339	-1509.022	46.44189
c_{10}	-0.0070535	0.001179	0.185319	0.005984
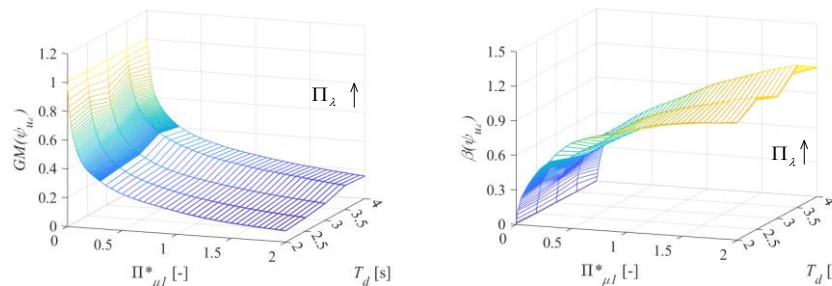
Fig. 3 Normalized deck displacement ψ_{u_d} vs. $\Pi^*_{\mu_1}$ and T_d for $T_p = 0.05s$ and for $\Pi_\lambda = 0.10, 0.15, 0.2$: left) mean value; right) dispersion.

4   CONCLUSIONS

This work studies the seismic performance of multi-span continuous deck bridges isolated with DCFP devices by adopting a simplified 8dof system. A wide range of isolator and bridge properties is investigated through non-dimensional parametric analysis, recording both the deck and pier maximum response. The uncertainty in the seismic input is considered by solving the equations of motion for a set of 30 different ground motions. The outcomes of the dynamic analyses have been then statistically treated by computing the geometric mean and coefficient of variation. This has allowed concluding that: regarding the pier performance, an optimal value for the sliding friction coefficient can be obtained by minimizing the pier maximum response, depending on the bridge and isolator properties; concerning the deck performance, the response decreases significantly as the sliding friction coefficient is larger.

REFERENCES

[1] Gino D., Castaldo P., Anerdi C., Ferrara M., Bertagnoli G. and Giordano L., 2020. "Seismic upgrading of existing reinforced concrete buildings using friction pendulum Devices: A Probabilistic Evaluation." Applied Sciences 10.24: 8980. doi:10.3390/app10248980
[2] Castaldo P., and Alfano G., 2020. "Seismic reliability-based design of hardening and softening structures isolated by double concave sliding devices." Soil Dyn. Earthq. Eng. 129: 105930.

[3]   Constantinou M., Kartoum A., Reinhorn A.M., and Bradford P., 1992. "Sliding isolation system for bridges." Experimental study, Earthquake Spectra, 8.3: 321-344.

[4]   Mancini G., Carbone V.I., Bertagnoli G., Gino D., 2018. "Reliability-based evaluation of bond strength for tensed lapped joints and anchorages in new and existing reinforced concrete structures." Structural Concrete 19.3: 904-917. https://doi.org/10.1002/suco.201700082

[5]   Tsopelas, P., Constantinou M., Okamoto S., Fujii S., and Ozaki D., 1996 "Experimental study of bridge seismic sliding isolation systems." Engineering Structures 18.4: 301-310.

[6]   Jangid, R.S. 2008. "Stochastic Response of Bridges Seismically Isolated by Friction Pendulum System." Journal of Bridge Engineering 13.4: 319-330. 2008.

[7]   Murat D., Buddaram S., 2006. "Effect of isolator and ground motion characteristics on the performance of seismic-isolated bridges." Earthquake engineering & structural dynamics 35.2: 233-250.

[8]   Zayas V.A., Stanley S.L., Mahin S.A., 1990. "A simple pendulum technique for achieving seismic isolation." Earthquake Spectra 6.2: 317–333.

[9]   Fenz, D.M., and Constantinou M., 2006. "Behaviour of the double concave friction pendulum bearing." Earthquake Engineering and Structural Dynamics 35.11: 1403-1424.

[10] Castaldo P., Amendola G. 2021. "Optimal sliding friction coefficients for isolated viaducts and bridges: A comparison study." Structural Control and Earthquake Engineering 2021, e2838.

[11] Constantinou, M., "Friction pendulum double concave bearings." Technical report University of Buffalo, NY, October 29, 2004.

[12] Kim, Y.S., Yun C.B.,.2007. "Seismic response characteristics of bridges using double concave friction pendulum bearings with tri-linear behavior." Engineering Structures 29.11: 3082-3093.

[13] Castaldo, P., Amendola, G. 2021. "Optimal DCFP bearing properties and seismic performance assessment in nondimensional form for isolated bridges." Earthquake Engineering and Structural Dynamics, 50(9), 2442-2461, DOI: 10.1002/eqe.3454.

[14] Kunde, M.C., Jangid R.S.. 2006. "Effects of pier and deck flexibility on the seismic response of isolated bridges." Journal of Bridge Engineering 11.1 109-121.

[15] Constantinou M,.; Kalpakidis I, Filiatrault A., Ecker Lay R.A., LRFD-Based Analysis and Design Procedures for Bridge Bearings and Seismic Isolators MCEER-11-0004

[16] Mokha, A., Constantinou M., Reinhorn A., 1990. "Teflon Bearings in Base Isolation I: Testing." Journal of Structural Engineering 116.2: 438-454.

[17] Constantinou, M, Mokha A., and Reinhorn A., 1990. "Teflon Bearings in Base Isolation II: Modeling." Journal of Structural Engineering 116.2: 455-474.

[18] Constantinou M., Whittaker A., Kalpakidis Y., Fenz D.M., Warn G.P., 2007. "Performance of Seismic Isolation Hardware Under Service and Seismic Loading." Technical Report No. MCEER-07.

[19] Castaldo, P., and Tubaldi E., 2018. "Influence of ground motion characteristics on the optimal single concave sliding bearing properties for base-isolated structures." Soil Dyn Earth Eng. 104: 346–364.

[20] Bertero, R.D., and Bertero, V.V., 2002. "Performance-based seismic engineering: the need for a reliable conceptual comprehensive approach." Earthq Eng Struct Dyn 31: 627–652.

[21] Shome, N., Cornell A.C.,Bazzurro P., and Carballo J.E., 1998. "Earthquake, records, and non-linear responses." Earthquake Spectra 14.3: 469-500.

[22] Castaldo P., Palazzo B., Ferrentino T., 2017. "Seismic reliability-based ductility demand evaluation for inelastic base-isolated structures with friction pendulum devices" Earthq Eng Struct Dyn 46.8.

[23] Aslani, H., and Miranda E., 2005. "Probability-based seismic response analysis." Engineering Structures 27.8: 1151-1163.

[24] Ang, Alfredo H.S., and Wilson H.T., 2007. "Probability Concepts in Engineering-Emphasis on Applications to Civil and Environmental Engineering." John Wiley & Sons Incorporated, New York, USA, 2007.

[25] Math Works Inc. MATLAB-High Performance Numeric Computation and Visualization Software. User's Guide. Natick: MA, USA, 1997.

KEYWORDS

Seismic isolation, double concave friction pendulum isolators, multi-span continuous deck bridges, performance-based engineering, non-dimensional form.